

Choroid changes in vortex vein-occluded monkeys

Lu-Lu Chen¹, Qiong Wang², Wei-Hong Yu¹, You-Xin Chen¹

¹Department of Ophthalmology, Peking Union Medical College Hospital, Chinese Academy of Medical Sciences, Beijing 100730, China

²Department of Nephrology, Beijing Hospital, Beijing 100730, China

Correspondence to: You-Xin Chen. Department of Ophthalmology, Peking Union Medical College Hospital, Chinese Academy of Medical Sciences, No.1 Shuaifuyuan Wangfujing Dongcheng District, Beijing 100730, China. chenyouxinpumch@163.com

Received: 2018-03-31 Accepted: 2018-08-03

Abstract

• **AIM:** To determine acute and chronic choroidal vascular changes after vortex vein occlusion in monkeys.

• **METHODS:** One or two temporal vortex veins were occluded in 8 cynomolgus monkeys. Fluorescein angiography (FA), indocyanine green angiogram (ICGA), and enhanced-depth imaging optical coherence tomography (EDI-OCT) were performed preoperatively and at 1d, 1, 4, 8 and 12wk after occlusion. EDI-OCT images were binarized to calculate the choroid vascular index (CVI).

• **RESULTS:** ICGA showed delayed filling of choroidal arteries in occluded quadrants in eyes with two occluded temporal vortex veins within 1wk. The thickness of the superotemporal choroid increased 1d and 4wk after occlusion, the thickness of the superonasal and inferonasal choroid increased 12wk after occlusion, and the CVI of the superonasal quadrant increased 8wk after occlusion in eyes with 2 occluded vortex veins.

• **CONCLUSION:** Occlusion of two vortex veins leads to hemodynamic and structural changes in choroidal layers in the acute phase, while autoregulation may play the main role in the long term. Occlusion of one vortex vein has little influence on the hemodynamic and structural status of the choroid.

• **KEYWORDS:** vortex vein occlusion; choroidal circulatory disturbance; cynomolgus monkey

DOI:10.18240/ijo.2018.10.03

Citation: Chen LL, Wang Q, Yu WH, Chen YX. Choroid changes in vortex vein-occluded monkeys. *Int J Ophthalmol* 2018;11(10):1588-1593

INTRODUCTION

Pachychoroid, characterized by choroidal vessel dilatation, is a broad term that implicates structural and/or functional choroidal alteration as a key pathophysiological mechanism in a range of disorders^[1-3]. Recent studies tend to categorize diseases such as polypoidal choroidal vasculopathy, pigment epitheliopathy, and central serous chorioretinopathy into the spectrum of pachychoroidal diseases^[4-7]. The pathogenic mechanism that accounts for dilated choroidal vessels and pachychoroid remains unclear, but current research has determined that these changes are secondary to choroidal venous congestion. The choroid comprises 3 vascular layers from internal to external. The inner layer is the choriocapillaris, the middle layer is Sattler's layer, and the outer layer is Haller's layer, which are arranged with increasing luminal diameter. Vortex veins are the main drainage routes for choroidal vessels. There are 1-2 vortex veins in each quadrant of the human eye, and each vortex vein has a well-defined segmental distribution, dividing the uveal venous system into four functionally independent segments^[8]. Hayreh and Baines^[9] conducted experimental occlusion of vortex veins in rhesus monkeys and found marked venous congestion and sluggish circulation in the affected segments of the uveal tract. Nishikawa *et al*^[10] observed delay of choroidal artery filling and clearance in indocyanine green angiograms (ICGAs) of occluded eyes in the acute phase in Japanese macaque monkeys. However, the detailed acute and chronic changes in choroidal layers remain unknown. The choroid vascular index (CVI) is a term proposed to assess the vascularity of the choroid based on an image binarization technique. The development and application of this parameter has been thoroughly described in various studies in recent years^[11-16]. The CVI and image binarization method can provide a detailed examination of choroidal vascular changes. The purpose of this study was to determine acute and chronic choroidal vascular changes after vortex vein occlusion. To accomplish this purpose, we occluded one or two vortex veins in 8 cynomolgus monkeys and thoroughly examined changes with fluorescein angiography (FA), ICGA, and enhanced-depth imaging optical coherence tomography (EDI-OCT).

SUBJECTS AND METHODS

Sixteen eyes of 8 cynomolgus monkeys, each aged 3-5 years old and weighing 3-5 kg, were studied. Research on cynomolgus monkeys followed the guidelines of the ARVO

Statement for the Use of Animals in Ophthalmic and Vision Research, adhered to the tenets of the Declaration of Helsinki for the use of animals in research and was approved by the Institutional Animal Care and Use Committee (IACUC) review board (ACU17-090). The animal experiments also conformed to institutional standards.

All subjects underwent complete ophthalmic examinations, including indirect ophthalmoscopy, color fundus photographs, noncontact intraocular pressure (IOP), EDI-OCT, FA, and ICGA. No significant abnormalities were observed in any of the eyes preoperatively.

Induction of Experimental Vortex Vein Ligation Animals were equally divided into two groups (Groups A and B), and one eye of each animal was randomly selected as the operation eye, while the other served as a control. The animals were sedated with intramuscular injection of 4-12 mg/kg (50 mg/mL) Zoletil 50 (Virbac, France), followed by pupillary dilation with tropicamide. Two vortex veins from the superotemporal and inferotemporal quadrants of the operation eye in subjects in group A were isolated and completely ligated with 6-0 non-absorbable sutures. One inferotemporal vortex vein was ligated in the operation eye of each monkey in group B. The bulbar conjunctiva was incised to expose the vortex veins and then closed in all control eyes. Noncontact IOP was measured within 10min after surgery.

Fluorescein Angiography and Indocyanine Green Angiogram FA and ICGA were performed preoperatively and at 1d, 1, 4, 8 and 12wk post-surgery using a laser scanning ophthalmoscope (Micro Clear, China). We administered 0.2 mL/kg of 5% sodium fluorescein or 2.5 mg/kg of indocyanine green (ICG) intravenously at each attempt. FA was performed first and required 5min to complete. Next, ICGA was performed and required approximately 30min for each eye. A 30-minute break was taken before ICG was performed on the second eye of the subject. Videos of the first minute of FA and ICG were recorded, and pictures of the angiograms were taken every 15s after 1min.

Enhanced-depth Imaging Optical Coherence Tomography EDI-OCT was performed using a Spectralis SD-OCT device (Heidelberg Engineering, Germany) with a 30°×20° horizontal line scan with 100 frames averaged in each B scan. The scanning areas were centered on the fovea and four quadrants surrounding the optic disc.

Analysis of Indocyanine Green Angiogram

Indocyanine green filling pattern The filling pattern of ICG in the operated quadrants and non-operated quadrants was read by two independent researchers (Chen LL and Wang Q) who had undergone standard training in ICG reading. The researchers decided whether there was a delay in ICG filling in the operated quadrant. If the results from both researchers agreed, they were accepted. If not, a third senior researcher (Chen YX) made the final decision.

Indocyanine green outflow clearance time The time from intravenous injection of ICG to the disappearance of dye in choroidal veins was defined as the ICG outflow clearance time. Two researchers independently determined the outflow clearance time (Chen LL, Wang Q), and the average of both measurements was the final ICG outflow clearance time.

OCT Image Analysis

Choroidal thickness Choroidal thickness was measured by two independent researchers (Chen LL and Wang Q), and the average thickness was determined as choroidal thickness. Choroidal thickness was defined as the distance between Bruch's membrane [lower boundary of the retinal pigmented epithelium (RPE)] and the choroidal-scleral interface. The choroidal thickness of the subfoveal area and areas located 3800 μm from the optic disc in each quadrant (superotemporal, superonasal, inferotemporal and inferonasal) were measured.

Choroid vascular index OCT images were selected for binarization. The binarization protocol was described by Sonoda *et al*^[11] and modified by Agrawal *et al*^[13]. We applied the protocol of Agrawal *et al*^[13]. Image binarization was performed by a modified Niblack method using public domain software, Fiji (<https://imagej.net/ImageJ>). Images were uploaded on Fiji and converted to 8-bit images to allow the application of auto local threshold. The horizontal scale on OCT scans was used to convert pixels to microns. The selected examined area was 1000 μm wide, with margins 500 μm nasal and 500 μm temporal to the fovea or the selected site surrounding the optic nerve head in each quadrant. The area extended from the RPE to the chorio-scleral border, and this area was then set with the ROI Manager. The choroidal area was segmented, and the total subfoveal choroidal area (TCA) was computed. Brightness was reduced to clearly visualize choroidal vessels and minimize the noise in EDI-OCT images. Agrawal *et al*^[13] previously found that Niblack auto local threshold provides the best resolution and demarcation of luminal area (LA), *i.e.* the dark part, and stromal area (SA), *i.e.* the bright part; thus, it was applied to all images (Figure 1).

Inter-rater and intra-rater agreement A set of 36 images were initially processed by two researchers (Chen LL and Wang Q) to determine inter-rater agreement. The same set of images was processed by one researcher (Chen LL) after an interval of one week to compute intra-rater reliability. The intra- and inter-rater reliability for the measurement of images was measured by the absolute agreement model of intra-class correlation fair agreement. An intraclass correlation coefficient (ICC) value of 0.81-1.00 indicates good agreement. Values less than 0.40 indicate poor to fair agreement. After obtaining good inter- and intra-rater agreement, all images were processed by a single researcher (Chen LL).

Statistical Analysis Statistical analysis was performed using SPSS version 24.0 (SPSS, Inc., Chicago, IL, USA). Significant

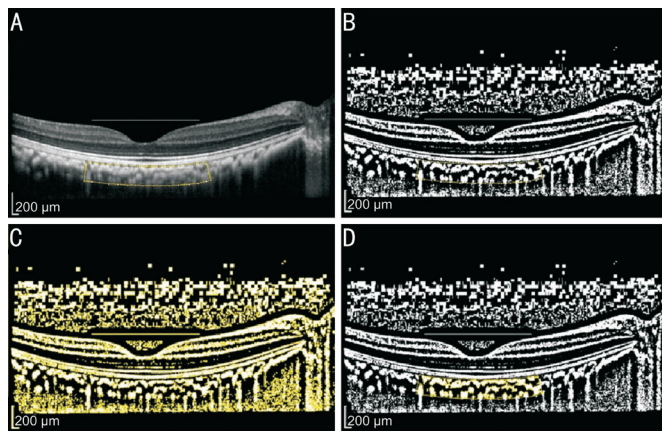


Figure 1 Image binarization for subfoveal choroid A: Original EDI-OCT image with selected region of interest (ROI); B: Binarized EDI-OCT image. Dark area representing luminal area and white area representing interstitial area; C: Red, green, blue (RGB) image. Dark area selected; D: Overlay image of the choroid was created in ROI.

differences between two groups at each check point were determined by paired *t*-test of equal variance. Differences in the same group at different check points were compared using one-way ANOVA. A *P* value <0.05 was considered significant.

RESULTS

Appearance of Eyes After Occlusion Aqueous flare and hyphema were observed in the anterior chamber within 15min after ligation of vortex veins but disappeared after one week. The mean IOP of the surgery eye increased to 29.50 ± 7.76 mm Hg from a preoperative IOP of 10.00 ± 0.81 mm Hg in group A, while the IOP of the control eyes remained stable (13.50 ± 3.42 mm Hg vs 10.00 ± 0.82 mm Hg). The post-operative IOP increased to 16.50 ± 1.91 mm Hg from a baseline of 9.50 ± 0.58 mm Hg in group B, and the IOP in the control eyes was not significantly different (10.50 ± 1.73 mm Hg vs 9.50 ± 0.58 mm Hg). IOP in surgery eyes returned to baseline level in both groups within 3d after surgery.

Fluorescein Angiography Patchy hyperfluorescence was observed in superotemporal and inferotemporal areas in one occluded eye in group A one day after occlusion. These hyperfluorescent areas disappeared after one week (Figure 2). FA of other occluded eyes showed no filling defect or leakage from retinal vessels and did not differ significantly from the preoperative images.

Indocyanine Green Angiogram Filling Pattern

Group A In the early phase, ICGAs showed delayed filling of choroidal arteries in occluded quadrants in all occluded eyes within 1wk. Hypofluorescence was observed in temporal quadrants in the late phase. Notably, relatively hyperfluorescent dots were observed in the late phase of the ICGA in one occluded eye one day after surgery, while delayed filling was detected in the same areas after 4wk (Figure 3). No significant difference was observed in control eyes.

Group B There was no significant difference between the ICGA of occluded eyes and the ICGA of eyes preoperatively and control eyes.

Indocyanine Green Outflow Clearance Time

Group A The ICG outflow clearance time did not differ significantly after vortex vein occlusion in both occluded eyes and control eyes. The mean ICG outflow clearance time in occluded eyes was 772.25 ± 209.07 s preoperatively and 832.00 ± 117.79 s 12wk postoperatively.

Group B No significant differences in the ICG outflow clearance time were observed in both occluded eyes and control eyes.

Choroidal Thickness In group A, the superotemporal choroid was thicker in operative eyes than in control eyes 1d and 4wk after surgery (1d after surgery: 218.1 ± 23.7 μ m vs 172.5 ± 35.8 μ m, *P*=0.025; 4wk after surgery: 206.3 ± 26.4 μ m vs 183.0 ± 34.2 μ m, *P*=0.013). The superonasal and inferonasal choroid were thicker in surgery eyes than in control eyes 12wk after surgery (superonasal choroid thickness 12wk after surgery: 150.8 ± 48.3 μ m vs 138.8 ± 48.0 μ m, *P*=0.016; inferonasal choroid thickness 12wk after surgery: 149.5 ± 44.8 μ m vs 127.0 ± 38.8 μ m, *P*=0.045).

The superotemporal choroid in surgery eyes was thicker 1d to 8wk after surgery than before surgery (1d 218.1 ± 23.7 μ m, *P*=0.008; 1wk 219.0 ± 39.4 μ m, *P*=0.007; 4wk 206.3 ± 26.4 μ m, *P*=0.032; 8wk 203.5 ± 11.2 μ m, *P*=0.044; preoperative 165.5 ± 25.5 μ m). The choroidal thickness of the macular area was thicker 1d after surgery than before surgery in the operative eye (173.8 ± 11.6 μ m vs 218.9 ± 4.4 μ m, *P*=0.022). Choroidal thickness in control eyes remained stable.

In group B, the superotemporal choroid was thicker in surgery eyes 1wk after surgery than in control eyes (183.0 ± 30.1 μ m vs 167.8 ± 31.4 μ m, *P*=0.007).

There was no difference between the choroidal thickness of all five sites in surgery eyes post-surgery and preoperatively. Choroidal thickness was unchanged in control eyes.

Choroid Vascular Index Using image binarization, the inter-rater agreement for TCA was very high, with an ICC of 0.940. The ICCs were also high for the luminal and interstitial areas (0.956-0.975).

The intra-class agreement for TCA was also very high, with the ICC of 0.955. ICCs were also high for the luminal and interstitial areas (0.965-0.980; Table 1).

In group A, the CVI was higher in the superonasal quadrant in operative eyes than in control eyes 8wk after surgery ($59.57\% \pm 4.43\%$ vs $56.90\% \pm 4.16\%$, *P*=0.027).

The CVI in operative eyes was higher in the superotemporal quadrant 4wk and 8wk after surgery than before surgery (4wk: $61.14\% \pm 3.79\%$, *P*=0.033; 8wk: $61.06\% \pm 2.98\%$, *P*=0.035; preoperative: $56.39\% \pm 2.41\%$). The CVI was stable in control eyes.

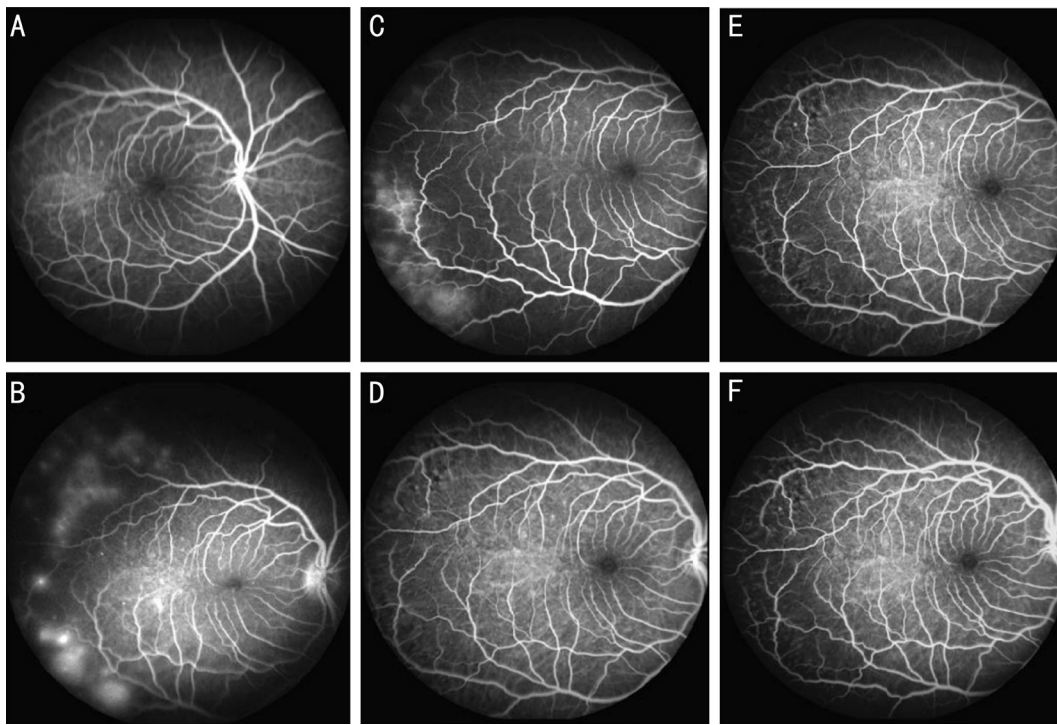


Figure 2 FA for one monkey with two occluded temporal vortex veins A: Normal fundus FA image before surgery; B: Patchy hyperfluorescence in superotemporal and inferotemporal areas in one occluded eye 1d after occlusion; C: Patchy hyperfluorescent areas appeared in same area 1wk after vortex vein occlusion. These hyperfluorescent areas disappeared at 4wk (D), 8wk (E) and 12wk (F) after surgery.

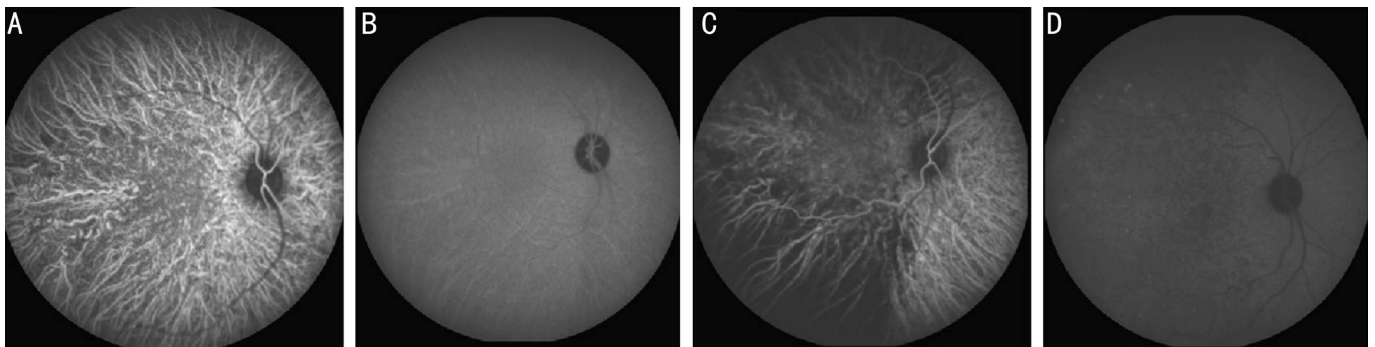


Figure 3 ICG for one monkey with two occluded temporal vortex veins A: Normal filling of choroid vessels; B: Late phase ICGA before surgery; C: Delay of choroid filling in temporal quadrants 1d after surgery; D: Hyperfluorescent dots appeared in superotemporal quadrant and hypofluorescent in temporal quadrants in late phase.

Table 1 Intra- and inter-grader reliability assessment of choroidal parameters

Parameters	Interclass ICC	95%CI	Intraclass ICC	95%CI
TCA (μm^2)	0.940	0.881-0.969	0.955	0.912-0.977
LA (μm^2)	0.956	0.914-0.978	0.965	0.930-0.982
SA (μm^2)	0.975	0.933-0.989	0.980	0.961-0.990
CVI	0.969	0.824-0.989	0.986	0.972-0.993

TCA: Total subfoveal choroidal area; LA: Luminal area; SA: Stromal area; ICC: Intraclass correlation coefficient; CI: Confidence interval.

In group B, there was no difference in the CVI between operative eyes and control eyes after surgery. Moreover, there was no difference in the CVI between operative eyes before and after surgery. The CVI in control eyes remained stable.

DISCUSSION

Our results demonstrated that occluding two vortex veins

altered the filling pattern and structures of choroidal vessels. The filling of choroidal vessels in the field of occluded vortex veins in ICGAs was delayed. The choroidal thickness of the occluded regions increased after ligation and then returned to baseline levels, while the choroidal thickness of non-occluded areas increased. Compared with choroidal thickness, CVIs

showed a similar pattern of changes. However, occlusion of one vortex vein has little influence on the hemodynamic and structural status of the choroid.

The IOP increased to approximately 30 mm Hg in eyes with two occluded vortex veins within 10min but returned to baseline level within 3d. High IOP might cause a reduction in perfusion pressure, but it was insufficient to alter the FA and ICGA in the non-occluded area of the choroid. This finding indicated that the changes in the ICGA in the occluded area most likely did not result from the decrease in perfusion pressure.

Choroidal vessel filling occurred simultaneously in all four quadrants before surgery, while delayed filling was prominent in occluded fields after ligation. This finding was similar to previous research by Nishikawa *et al*^[10] who suggested that occlusion of the vortex veins resulted in an acute increase in venous pressure that led to a delay in vessel filling. Our study also showed that this delayed filling lasted for 1wk only; this result suggested that vortex vein ligation disturbed choroidal blood flow in the acute phase that was eventually compensated for. Moreover, in Nishikawa *et al*'s^[10] study, delayed clearance of ICG dye was found uniformly in all quadrants in the occluded eye, suggesting that stagnant venous blood was drained equally through anastomoses to the non-occluded vortex veins. However, there was no significant difference in ICG clearance time in our study. Many potential reasons could account for these discrepant results. Nishikawa *et al*^[10] conducted ICGA 30min after ligation, while we conducted ICGA 1d after ligation in our study. Delayed dye clearance could be most prominent during acute occlusion and then gradually compensated by the regulation of related vessels. Additionally, anesthetic status could exert some influence on blood flow rate.

Interestingly, patchy hyperfluorescence in FA was observed in occluded areas in one eye with two ligated vortex veins within 1wk after surgery. Relative hyperfluorescent dots were also observed in the late phase of ICGA during the same time period after surgery. Delayed filling of choroidal vessels in these areas was observed 4wk after ligation. Hayreh and Banies^[9] reported that vortex vein ligation results in sluggish flow in the choroidal circulation and patchy perfusion in the field of occluded areas. Although there were some differences between our results and theirs, these results revealed that vortex vein occlusion disturbed the circulation of choroidal vessels. We assumed that the hemodynamics of occluded fields was disturbed after surgery, and the sudden change in intravascular pressure would result in damage to the microenvironment of the microvasculature, leading to leakage of dye in the acute phase. As occlusion persisted, blood would be drained by non-occluded veins or anastomoses through the unaffected field.

Here, the choroidal thickness of the superotemporal field

increased transiently after occlusion of 2 vortex veins. Interestingly, the choroidal thickness of the non-occluded areas increased 12wk after occlusion in group A. A previous histological study by Nishikawa *et al*^[10] proved that acute ligation of vortex veins can result in choroidal thickening, vessel dilatation and blood cell stagnancy in the occluded field. Takahashi and Kishi^[17] reported the remodeling of drainage routes that connected the sector of occluded vortex veins to that of intact vortex veins with venovenous anastomoses. Assuming that vortex vein ligation resulted in congestion of choroidal veins, which presented as choroidal thickening in the occluded field in the short term, was reasonable. However, as occlusion persisted, dilatation of choroidal vessels in the occluded area decayed, and venovenous anastomoses formed to make a new drainage route to choroidal veins connected to intact vortex veins.

The next question is whether there were any changes in the structure of the choroid. Previously, Sonada *et al*^[11-12] proposed a binarization technique to differentiate the luminal and interstitial components of the choroid in EDI-OCT images with publicly accessible software, ImageJ. Agrawal *et al*^[16] applied a modified version of Sonoda's protocol and proved the high validity and reproducibility of their protocol. The authors proposed an OCT-based metric termed "CVI" to assess the vascularity of the choroid and suggested that the CVI was influenced by fewer physiologic factors and was a potentially more stable index for the study of changes in the choroid. The ICC values for TCA, LA, and SA for inter- and intra-class agreement in our research all exceeded 0.90, similar to reported previously reported values^[13,16,18], indicating that the CVI is a reliable parameter.

In our study, the CVI in the superotemporal quadrant increased after occlusion of 2 vortex veins, indicating choroidal vessel dilatation. Moreover, the CVI in the superonasal area increased 8wk after surgery. This result suggested increased drainage of blood through this region of the choroid, and it was reasonable for us to suspect remodeling of choroidal vessels and venovenous anastomoses 8wk after the occlusion of vortex veins. We also noticed that changes in the CVI were not synchronized with changes in choroidal thickness. Changes in choroidal thickness were more easily detected. We suggested that choroidal thickening was caused by both dilated vessels and accumulation of exudates from congested vessels. The CVI reflected the proportion of vessel area in one cross-sectional image. Increments in vessel area accompanied by increments in SA resulted in a relatively stable CVI.

However, no changes in choroidal thickness and CVIs were observed when only one vortex vein was occluded. Evidence from animal and human studies has shown a certain degree of autoregulation in the choroidal system^[19-21]. The dilatation of choroidal vessels may be limited due to autoregulation, and

hemodynamic changes in blood flow may be well tolerated when only one vortex vein is occluded.

Our study has some limitations. First, the sample size of each group was small. Each individual exhibited variations in choroid structure. We processed 2-dimensional EDI-OCT images with a binarization method to obtain CVIs representing regions of interest, but changes in the choroid layer occurred in a 3-dimensional manner, which was beyond our measurement capabilities. In future studies, 3-dimensional analysis of choroid structure will provide better understanding of changes in the choroid layer.

In conclusion, occlusion of vortex veins leads to hemodynamic and structural changes in choroid layers in the acute phase, while autoregulation may play the main role in the long term. Occlusion of one vortex vein has little influence on the hemodynamic and structural status of the choroid.

ACKNOWLEDGEMENTS

Foundation: Supported by National Natural Science Foundation of China (No.81670879).

Authors' contributions: Design of the study (Chen LL, Wang Q, Chen YX), animal surgery (Yu WH), collection (Chen LL, Wang Q), analysis (Chen LL, Wang Q), interpretation of data (Chen LL), writing (Chen LL), revision and editing (Chen YX).

Conflicts of Interest: Chen LL, None; Wang Q, None; Yu WH, None; Chen YX, None.

REFERENCES

- 1 Gallego-Pinazo R, Dolz-Marco R, Gomez-Ulla F, Mrejen S, Freund KB. Pachychoroid diseases of the macula. *Med Hypothesis Discov Innov Ophthalmol* 2014;3(4):111-115.
- 2 Dansingani KK, Balaratnasingam C, Klufas MA, Sarraf D, Freund KB. Optical coherence tomography angiography of shallow irregular pigment epithelial detachments in pachychoroid spectrum disease. *Am J Ophthalmol* 2015;160(6):1243-1254.e1242.
- 3 Balaratnasingam C, Lee WK, Koizumi H, Dansingani K, Inoue M, Freund KB. Polypoidal choroidal vasculopathy: a distinct disease or manifestation of many? *Retina* 2016;36(1):1-8.
- 4 Pang CE, Freund KB. Pachychoroid neovasculopathy. *Retina* 2015; 35(1):1-9.
- 5 Warrow DJ, Hoang QV, Freund KB. Pachychoroid pigment epitheliopathy. *Retina* 2013;33(8):1659-1672.
- 6 Kuroda S, Ikuno Y, Yasuno Y, Nakai, K, Usui, S, Sawa, M, Tsujikawa, M, Gomi, F, Nishida, K. Choroidal thickness in central serous chorioretinopathy. *Retina* 2013;33(2):302-308.
- 7 Yun C, Han JY, Cho S, Hwang SY, Kim SW, Oh J. Ocular perfusion pressure and choroidal thickness in central serous chorioretinopathy and pigment epitheliopathy. *Retina* 2017.

- 8 Hayreh SS. Segmental nature of the choroidal vasculature. *Br J Ophthalmol* 1975;59(11):631-648.
- 9 Hayreh SS, Baines JA. Occlusion of the vortex veins. An experimental study. *Br J Ophthalmol* 1973;57(4):217-238.
- 10 Nishikawa M, Matsunaga H, Takahashi K, Matsumura M. Indocyanine green angiography in experimental choroidal circulatory disturbance. *Ophthalmic Res* 2009;41(1):53-58.
- 11 Sonoda S, Sakamoto T, Yamashita T, Shirasawa M, Uchino E, Terasaki H, Tomita M. Choroidal structure in normal eyes and after photodynamic therapy determined by binarization of optical coherence tomographic images. *Invest Ophthalmol Vis Sci* 2014;55(6):3893-3899.
- 12 Sonoda S, Sakamoto T, Yamashita T, Uchino E, Kawano H, Yoshihara N, Terasaki H, Shirasawa M, Tomita M, Ishibashi T. Luminal and stromal areas of choroid determined by binarization method of optical coherence tomographic images. *Am J Ophthalmol* 2015;159(6):1123-1131.e1121.
- 13 Agrawal R, Salman M, Tan KA, Karampelas M, Sim DA, Keane PA, Pavesio C. Choroidal vascularity index (CVI)-a novel optical coherence tomography parameter for monitoring patients with panuveitis? *PLoS One* 2016;11(1):e0146344.
- 14 Agrawal R, Wei X, Goud A, Vupparaboina KK, Jana S, Chhablani J. Influence of scanning area on choroidal vascularity index measurement using optical coherence tomography. *Acta Ophthalmol* 2017;95(8):e770-e775.
- 15 Bakthavatsalam M, Ng DS, Lai FH, Tang FY, Brelén ME, Tsang CW, Lai TY, Cheung CY. Choroidal structures in polypoidal choroidal vasculopathy, neovascular age-related maculopathy, and healthy eyes determined by binarization of swept source optical coherence tomographic images. *Graefes Arch Clin Exp Ophthalmol* 2017;255(5): 935-943.
- 16 Agrawal R, Gupta P, Tan KA, Cheung CM, Wong TY, Cheng CY. Choroidal vascularity index as a measure of vascular status of the choroid: measurements in healthy eyes from a population-based study. *Sci Rep* 2016;6:21090.
- 17 Takahashi K, Kishi S. Remodeling of choroidal venous drainage after vortex vein occlusion following scleral buckling for retinal detachment. *Am J Ophthalmol* 2000;129(2):191-198.
- 18 Agrawal R, Chhablani J, Tan KA, Shah S, Sarvaiya C, Banker A. Choroidal vascularity index in central serous chorioretinopathy. *Retina* 2016;36(9):1646-1651.
- 19 Kiel JW, Shepherd AP. Autoregulation of choroidal blood flow in the rabbit. *Invest Ophthalmol Vis Sci* 1992;33(8):2399-2410.
- 20 Kiel JW. Choroidal myogenic autoregulation and intraocular pressure. *Exp Eye Res* 1994;58(5):529-543.
- 21 Fuchsjäger-Mayrl G, Luksch A, Malec M, Polska E, Wolzt M, Schmetterer L. Role of endothelin-1 in choroidal blood flow regulation during isometric exercise in healthy humans. *Invest Ophthalmol Vis Sci* 2003;44(2):728-733.